Macromolecules

ARTICLE

pubs.acs.org/Macromolecules

# Microphase Separation Mode-Dependent Mechanical Response in Poly(vinyl ester)/PEO Triblock Copolymers

Corinne E. Lipscomb and Mahesh K. Mahanthappa*

Department of Chemistry, University of Wisconsin—Madison, 1101 University Ave., Madison, Wisconsin 53706, United States

Supporting Information

**ABSTRACT:** The morphology and mechanical properties of a series of poly(vinyl ester)/poly(ethylene oxide) triblock copolymers are reported. Reversible addition−fragmentation chain transfer (RAFT) polymerizations of vinyl ester monomers mediated by an α,ω-telechelic poly(ethylene oxide) bearing terminal xanthate functionalities enable the bidirectional syntheses of monodisperse POP, AOA, and BOB (P = poly(vinyl pivalate); A = poly(vinyl acetate); B = poly(vinyl benzoate); O = poly(ethylene oxide)) triblock copolymers. By controlling the extent of monomer conversion in these RAFT polymerizations using a single difunctional macro-RAFT chain transfer agent having $M_{n,O}$ = 11.3 kg/mol, a series of polymers having O mass fractions 0.25 ≤ $w_O$ ≤ 1.00 and $M_{n,total}$ = 14.9−45.1 kg/mol ($M_w/M_n$ < 1.40) were synthesized. Through a combination of differential scanning calorimetry (DSC) and variable-temperature small-angle X-ray scattering (SAXS) analyses, the three triblock series are shown to exhibit three different solid-state morphologies that arise directly from (i) O crystallization from a microphase-separated melt, (ii) O crystallization-induced segregation, and (iii) complete suppression of O crystallization. The mechanical properties of these materials are correlated with the observed mode of microphase separation.

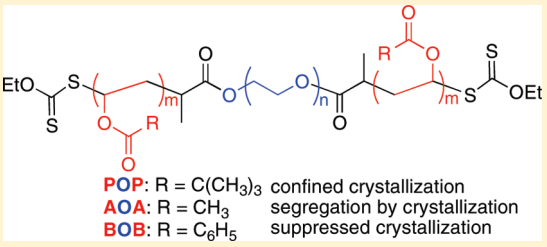


## INTRODUCTION

Concerns over the use and disposal of nondegradable polymers along with government mandates related to the incorporation of environmentally degradable materials into durable consumer goods have spurred the development of inexpensive, degradable polymers with widely tunable physical properties and processabilities.[1,2] While a majority of these research efforts have focused on (bio)degradable homopolymers and methods for toughening them to serve as surrogates for poly(olefins) and other widespread polymers,[3−5] increasing attention has focused on the development of degradable thermoplastics, thermoplastic elastomers, and pressure-sensitive adhesives.[6−10] Many of these studies describe copolymers containing cleavable ester, amide, and carbonate linkages in the main chain, including peptide materials that mimic natural silk.[11−16] The relatively high costs associated with many of these materials coupled with their limited processabilities and physical properties[5,17] motivate development of new classes of degradable block copolymers.

Available on commodity scales via metal-catalyzed oxidative coupling of ethylene and carboxylic acids, vinyl esters undergo free radical polymerization to yield poly(vinyl ester) (PVE) homopolymers (e.g., poly(vinyl acetate)) that find applications in paper-sizing, adhesives, food additives, and biomedical devices.[18] In spite of their all carbon backbone, PVEs chemically degrade under mild conditions by ester hydrolysis to carboxylic acids and poly(vinyl alcohol),[19] the latter of which is known to degrade into acetaldehyde and other small molecules.[20,21] Since the properties of these polymers depend sensitively on the structure of the ester, a variety of glassy, semicrystalline, and rubbery PVE homopolymers are known.[18] Thus, vinyl esters potentially comprise a monomer palette for the synthesis of cheap, degradable PVE block copolymers that potentially could exhibit useful thermoplastic or elastomeric properties for use in both commodity and specialty applications. As a step toward this goal, we recently reported the first PVE diblock copolymers using degenerate transfer polymerization techniques and demonstrated their microphase separation at intermediate molecular weights.[22−24]

In our studies of PVE block copolymers, we observed that microphase-separated triblock copolymers such as poly(vinyl benzoate-*b*-vinyl acetate-*b*-vinyl benzoate) are quite brittle.[25,26] Well-known design criteria for styene/diene block copolymer thermoplastics and thermoplastic elastomers indicate that block copolymers with glassy−rubbery−glassy block sequences typically exhibit large elastic moduli and high strength, if they microphase separate and if the rubbery midblock is entangled.[27−30] Microphase separation serves to physically cross-link the material by anchoring the glassy polymer chain ends in dispersed microdomains, thus maintaining trapped entanglements in the rubbery midblock that can bear mechanical loads.[30−36] We thus attribute the observed brittleness of our PVE triblock copolymers to the relatively high entanglement molecular weight and high glass transition temperature of the poly(vinyl acetate) center blocks ($M_e$ ∼ 8.5 kg/mol, $T_g$ ∼ 25-40 °C[37]). On the basis of the aforementioned design principles for high strength polydiene block copolymers, we sought to incorporate low entanglement molecular weight

**Received:** January 7, 2011
**Revised:** March 25, 2011
**Published:** May 06, 2011

and low glass transition temperature poly(ethylene oxide) segments ($M_e \sim 1.7$ kg/mol, $T_g \sim -60$ °C[37]) into these poly(vinyl esters) to toughen these polymers, while retaining the biocompatibility and potential degradability of the corresponding segments.[18,38]

Herein we report the bidirectional RAFT synthesis and complete molecular characterization of a homologous series of hybrid block copolymers comprised of poly(ethylene oxide) center segments flanked by glassy poly(vinyl ester) end blocks, including POP, AOA, and BOB (P = poly(vinyl pivalate), A = poly(vinyl acetate), B = poly(vinyl benzoate), and O = poly(ethylene oxide)). Using a combination of differential scanning calorimetry, variable temperature small-angle X-ray scattering, and uniaxial tensile measurements, we show that these triblock copolymers undergo different modes of microphase separation that result in very different supramolecular morphologies and bulk mechanical properties.

## EXPERIMENTAL SECTION

**Materials.** All reagents were purchased from Sigma-Aldrich and used as received unless otherwise noted. Vinyl acetate (VAc) and vinyl pivalate (VPv) were distilled from $NaBH_4$ at ambient pressure, and vinyl benzoate (VBz) was distilled from $NaBH_4$ under full vacuum immediately prior to use. Free radical initiators, 2,2′-azobis(isobutyronitrile) (AIBN) and 1,1′-azobis(cyclohexane-1-carbonitrile) (V-40, Wako Chemicals), were recrystallized from methanol before use. 2-Bromopropionyl bromide was fractionally distilled, and triethylamine was distilled from $CaH_2$ prior to use. Potassium *O*-ethyl xanthogenate was purchased from TCI America. (Ethyl 2-propionyl)diphenylcarbamothioate (**2**) was synthesized according to literature procedures.[39,40]

$^1$H NMR spectra were recorded in $CDCl_3$ on Varian Unity Inova 500 and Bruker AC+ 300 spectrometers and were referenced relative to the residual protiated solvent peaks in the samples. Triblock copolymer compositions and overall molecular weights ($M_{n,NMR}$) were calculated from quantitative $^1$H NMR spectra of the copolymers using the absolute molecular weight of the O block derived from SEC.

Polydispersity indices ($M_w/M_n$) of of triblock copolymers were determined using a Viscotek GPCMax System equipped with two Polymer Laboratories Resipore columns (250 mm × 4.6 mm), a differential refractometer, a two angle-light scattering module (7° and 90°), a four-capillary differential viscometer, and a UV/vis detector. Tetrahydrofuran (THF) was used as the mobile phase at 30 °C with a flow rate of 1.0 mL/min. $M_w/M_n$ values for all triblock copolymer samples are reported against a conventional calibration curve was constructed based on 10 narrow molecular weight distribution polystyrene standards with $M_n$ in the range of 580−377 400 g/mol.

Absolute molecular weights of poly(ethylene oxide) (O) and poly(vinyl benzoate) (B) were determined using the above system with either $CHCl_3$ or THF as the mobile phase at 40 °C with a flow rate of 0.8 mL/min. Triple-detection calibration relied on a narrow molecular weight distribution polystyrene standard ($M_n$ = 86.7 kg/mol, $M_w/M_n$ = 1.06) and the refractive index increments ($dn/dc$) for the respective polymers. The $dn/dc$ for O and B homopolymers were determined by fitting the integrated refractive index detector response as a function of polymer sample concentration upon elution from the SEC system using $n(CHCl_3)$ = 1.446 and $n$(THF) = 0.398 at 40 °C; $dn/dc$ (PEO) = 0.0554 mL/g in $CHCl_3$ and $dn/dc$ (PVBz) = 0.1370 mL/g in THF at 40 °C.

**Synthesis of Difunctional Xanthate Macro-RAFT PEO (1).** The difuctional xanthate macro-RAFT PEO was synthesized in two steps from commercially available α,ω-dihydroxy PEO. A modified literature procedure was employed to synthesize α,ω-dibromo telechelic PEO (Br−PEO−Br):[41] PEO ($M_n$ = 11.3 kg/mol, $M_w/M_n$ = 1.06) (20.21 g, 4.0 mmol) was dissolved in anhydrous $CH_2Cl_2$ (100 mL) with $Et_3N$ (0.60 mL, 4.3 mmol). 2-Bromopropionyl bromide (0.52 mL, 4.9 mmol) was added at 22 °C, and the reaction mixture was stirred overnight. The resulting polymer was precipitated in cold hexanes, dissolved in $C_6H_6$, and filtered through Celite to remove $Et_3NHBr$, after which the difunctional PEO was reprecipitated in cold hexanes and freeze-dried from $C_6H_6$ (86% recovery). Quantitative conversion of alcohol end groups to α-bromopropionyl esters was confirmed by $^1$H NMR end-group analysis.

To produce α,ω-bis(xanthyl) telechelic PEO, Br−PEO−Br (12.52 g, 1.1 mmol) was dissolved in anhydrous $CH_2Cl_2$ (100 mL) and solid potassium *O*-ethyl xanthogenate (1.2 g, 7.5 mmol) was added. After stirring this reaction mixture overnight at 22 °C, the resulting polymer was precipitated into cold hexanes, dissolved in $C_6H_6$, and filtered through Celite. Polymer was precipitated in cold hexanes and freeze-dried from $C_6H_6$. Macro-RAFT PEO **1** was obtained with 85% recovery. Quantitative conversion of polymer end groups was confirmed by close agreement between $M_{n,NMR}$ = 11.0 kg/mol determined by $^1$H NMR end-group analysis and the absolute $M_{n,SEC}$ = 11.3 kg/mol ($M_w/M_n$ = 1.06) from SEC. $^1$H NMR (500 MHz, $CDCl_3$): $\delta$ (ppm) 4.63 (*q*, 4H, $SC(S)OCH_2CH_3$), 4.40 (*q*, 2H, $CHCH_3$), 4.29 (*m*, 4H, $CH_2OC(O)$), 3.5−3.8 (*m*, 980 H, $(CH_2CH_2O)_n$), 1.57 (*d*, 6H, $CHCH_3$), 1.24 (*t*, 6H, $C(S)OCHCH_3$).

**Representative Synthesis of Poly(vinyl pivalate-*b*-ethylene oxide-*b*-vinyl pivalate): POP-23-50.** **1** (1.00 g, 0.09 mol), $C_6H_6$ (9.7 mL), VPv (10 mL, 0.07 mol), and AIBN (0.02 mmol, 0.3 mL of 65.8 mM solution in $C_6H_6$) were combined in a 100 mL Schlenk tube. The reactants were degassed via three freeze−pump−thaw cycles and placed in a 60 °C oil bath for 25.5 h. Excess monomer was removed by coevaporation with THF (20 mL) and the isolated polymer was freeze-dried from $C_6H_6$. $M_{n,NMR}$ = 22.7 kg/mol, $M_w/M_n$ = 1.20 (from SEC against PS standards).

**Representative Synthesis of Poly(vinyl acetate-*b*-ethylene oxide-*b*-vinyl acetate): AOA-27-43.** **1** (1.00 g, 0.09 mmol), $C_6H_6$ (9.72 mL), VAc (10 mL, 0.11 mol), and AIBN (0.02 mmol, 0.28 mL of 63.3 mM solution in $C_6H_6$) were combined in a 100 mL Schlenk tube. The reactants were degassed via three freeze−pump−thaw cycles and placed in a 60 °C oil bath for 18 h. The resulting polymer was diluted with THF (20 mL) and precipitated in cold hexanes. The polymer was then redissolved in $CHCl_3$ and precipitated twice in cold hexanes before freeze-drying from $C_6H_6$. $M_{n,NMR}$ = 26.5 kg/mol, $M_w/M_n$ = 1.19 (from SEC against PS standards).

**Representative Synthesis of Poly(vinyl benzoate-*b*-ethylene oxide-*b*-vinyl benzoate): BOB-40-28.** **1** (1.00 g, 0.09 mmol), $C_6H_6$ (9.6 mL), VBz (10 mL, 0.07 mol), and V-40 (0.02 mmol, 0.40 mL of 53.2 mM solution in $C_6H_6$) were combined in a 100 mL Schlenk tube. The reactants were degassed via three freeze−pump−thaw cycles and placed in an 88 °C oil bath for 18.3 h. The resulting polymer was diluted with THF (20 mL) and precipitated in cold hexanes. The polymer was redissolved in $CHCl_3$, precipitated twice into cold hexanes, and then freeze-dried from $C_6H_6$. $M_{n,NMR}$ = 39.9 kg/mol, $M_w/M_n$ = 1.26 (from SEC against PS standards).

**Synthesis of Poly(vinyl benzoate).** In a 100 mL Schlenk tube, **2** (55.9 mg, 0.16 mmol), VBz (6.0 mL, 0.04 mol), and V-40 (8.0 mg, 0.03 mmol) were combined and degassed via three freeze−pump−thaw cycles. The tube was placed in an 88 °C oil bath for 3.3 h. This polymerization reaction was cooled to room temperature, diluted with THF, and precipitated into cold hexanes. The polymer was then redissolved in THF and precipitated into cold hexanes twice before freeze-drying from $C_6H_6$. Absolute $M_{n,SEC}$ = 17.1 kg/mol, $M_w/M_n$ = 1.21 (from SEC against PS standards).

**Sample Preparation.** Triblock copolymers sample plaques for thermal, morphological, and mechanical analyses were compression-molded at 200 °C at 1400 psi for 2 min in a Carver hydraulic melt press (Model 3851-0). Mechanical testing specimens were further vacuum annealed at 100 °C for 4−6 h to yield void free samples. A B/O homopolymer blend was prepared by codissolution in $C_6H_6$ as a common solvent followed by freeze-drying and compression molding as above.

**Scheme 1. Synthesis of Difunctional Xanthate Macro-RAFT Agent PEO 1**

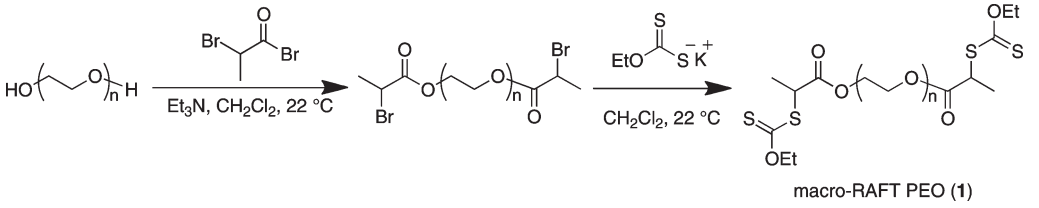


**Scheme 2. RAFT Synthesis of Poly(vinyl ester-*b*-ethylene oxide-*b*-vinyl ester) Triblock Copolymers**

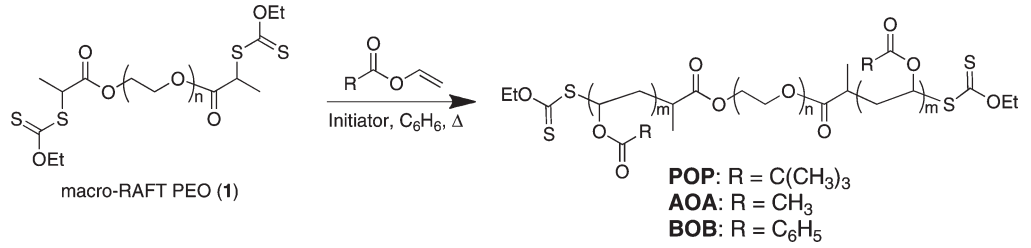


**Thermal Analysis.** Differential scanning calorimetry (DSC) was performed on a TA Instruments Q100A DSC and analyzed using the associated software. Glass transition temperatures ($T_{g,heat}$ and $T_{g,cool}$) determined by the midpoint method, peak melting and peak crystallization temperatures ($T_m$ and $T_c$), and enthalpies of melting ($\Delta H_{exp}$) of homopolymers and triblock copolymers were measured at a ramp rate of 5 °C/min from −60 to 100 °C for the first calorimetric cycle on compression-molded samples after 1 day of aging at 22 °C, unless otherwise specified. The crystalline weight fraction ($\chi_c$) was calculated using the theoretical heat of fusion for perfectly crystalline O ($\Delta H_{m,O}$ = 203 J/g[42]) and based on the O weight fraction ($w_O$) of the sample from

$$\chi_c = \frac{\Delta H_{exp}}{\Delta H_{m,O} w_O}$$

**Small-Angle X-ray Scattering (SAXS).** Cu Kα X-rays generated by a Rigaku Micromax 002+ microfocus source were collimated using a Max-Flux multilayer confocal optic (Osmic, Inc.) followed by passage through three collimating pinholes to reduce the final beam diameter to less than 0.5 mm. Samples were mounted in a vacuum chamber and heated using a Linkam hot stage using 15 min equilibration time at each temperature. A Gabriel X-ray detector (115 mm active circular area) was used to record 2D-SAXS patterns at a sample-to-detector distance of 2.015 m with typical exposure times ∼20 min.

**Mechanical Testing.** Mechanical analyses were carried out at room temperature using a Materials Testing Systems (MTS) Insight equipped with a MTS 2kN Advantage Grip Set and a 50 N load cell. Tensile bars having a thickness of 0.7 mm, width of 3.0 mm, and gauge length of 17.0 mm were tested using the MTS rectangular tension/compression mode using a crosshead speed of 0.2 mm/s (length-independent strain rate of 0.01 $s^{-1}$). Force−displacement measurements were converted to engineering stress $\sigma = F/A_0$ versus elongation $\varepsilon = (l - l_0)/l_0$, where $A_0$ and $l_0$ are the initial cross-sectional area and length, respectively. The elastic modulus, $E$, of each sample was determined by linearly fitting the stress−strain curve prior to the yield point. Reported data reflect an average of at least four independent trials.

## RESULTS

**Synthesis of Poly(vinyl ester-*b*-ethylene oxide-*b*-vinyl ester) Tribock Copolymers.** Difunctional xanthate macro-RAFT PEO **1** was synthesized in two steps from commercially available starting materials (Scheme 1). The alcohol end groups of α,ω-dihydroxy telechelic PEO ($M_n$ = 11.3 kg/mol, $M_w/M_n$ = 1.06) were esterified with 2-bromopropionyl bromide, using $Et_3N$ as a base *in lieu* of pyridine as previously reported to ease polymer purification.[41] The α-bromo ester end groups were subsequently reacted with potassium *O*-ethyl xanthogenate in $CH_2Cl_2$ to yield difunctional xanthate-terminated PEO **1** as a macromolecular RAFT chain transfer agent.

Triblock copolymers were synthesized by controlled RAFT polymerizations of VPv, VAc, or VBz mediated by bis(xanthate) **1** in $C_6H_6$ as a solvent (50% v/v solvent to monomer) with [**1**] = 5.0 mM and [**1**]:[initiator] = 0.2. AIBN-initiated VPv and VAc polymerizations were conducted at 60 °C, while polymerizations of VBz initiated with V-40 were run at 88 °C due to the higher temperature required for controlled polymerization of vinyl benzoate.[22] We note that AO diblock and AOA triblock copolymers have been previously synthesized under slightly different conditions; however, the melt morphology and solid-state behavior of these materials were not studied.[41,43,44] By controlling the extent of vinyl ester monomer conversion in these reactions, a series of poly(vinyl ester-*b*-ethylene oxide-*b*-vinyl ester) triblock copolymers having $M_{n,total}$ = 14.9−45.1 kg/mol and $M_w/M_n$ < 1.4 were synthesized (see Supporting Information Figure S1 for representative SEC traces). Poly(vinyl ester-*b*-ethylene oxide-*b*-vinyl ester) triblock copolymers are labeled according the convention XOX−Y−Z, wherein X designates the poly(vinyl ester) block (P, A, or B) and O designates the PEO segment with $M_n$ = 11.3 kg/mol and $M_w/M_n$ = 1.06, Y is $M_{n,total}$ for the sample in kg/mol, and Z is the mass fraction of O ($w_O$) in the sample. Molecular characteristics of POP, AOA, and BOB samples are enumerated in Tables 1−3, respectively.

**POP Triblock Copolymers.** Compression-molded samples of POP triblock copolymers were opaque and qualitatively quite brittle after 1 day of aging at 22 °C, thus motivating morphological analyses of these materials. Thermal analyses of these polymers reveal a substantial melting endotherm associated with the O block at $T_{m,O}$ ∼ 45−48 °C with modest crystallinities $\chi_c$ ∼ 0.45−0.59 upon heating, where $\chi_c$ decreases with decreasing $w_O$. While the


dx.doi.org/10.1021/ma200034u |*Macromolecules* 2011, 44, 4401–4409

**Table 1. Characterization Data for POP Triblock Copolymers**

| sample | $M_{n,P}$ (kg/mol)[a] | $M_{n,total}$ (kg/mol) | $M_w/M_n$ | $w_O$ | $T_{m,O}$ (°C)[b] | $T_{c,O}$ (°C)[c] | $T_g$ (°C)[d] | $\chi_c$ | morphology |
|---|---|---|---|---|---|---|---|---|---|
| O[e] | 0 | 11.3 | 1.06 | 1.00 | 58 | 40 | −53 | 0.79 | |
| POP-23-50 | 5.7 | 22.7 | 1.20 | 0.50 | 48 | 21 | n.o.[f] | 0.59 | dis |
| POP-31-37 | 9.8 | 30.9 | 1.24 | 0.37 | 45 | 14 | 48 | 0.50 | cyl |
| POP-45-25 | 16.9 | 45.1 | 1.39 | 0.25 | 48 | −25 | 61 | 0.45 | cyl |

[a] Present on each side of the O homopolymer segment. [b] $T_{m,O}$ = melting temperature of O block in the first heating cycle. [c] $T_{c,O}$ = crystallization temperature of O block in the first cooling cycle. [d] Observed $T_g$ upon cooling; the $T_g$ observed upon first heating cycle overlaps with the $T_{m,O}$. [e] Difunctional xanthate-terminated O homopolymer **1**. [f] Not observed.

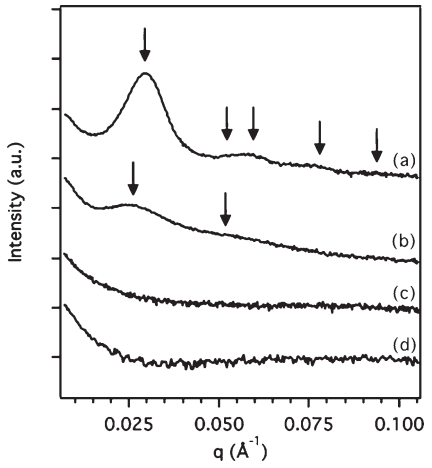


**Figure 1.** Azimuthally integrated intensity profiles of SAXS data acquired at 22 °C for (a) POP-45-25 indicating a cylindrical morphology (arrows indicate expected peak positions for the (100), (110), (200), (210), and (300) reflections) and (b) AOA-37-30 after 1 week of aging at 22 °C displaying of a lamellar morphology (arrows demarcate expected peak positions for the (001) and (002) reflections); apparently featureless scattering is observed from (c) AOA-37-30 after 1 day of aging at room temperature and (d) BOB-40-28 after 4 months aging. All data have been shifted vertically for clarity.

broad $T_g$ of the P block on heating is likely masked due to its proximity to the sharp melting transition of the semicrystalline O block, we clearly observe a $T_g \sim 47-61$ °C upon cooling (see Supporting Information Figures S2 and S3). We attribute this $T_g$ in POP-31-37 and POP-45-25 to that of the P blocks, given the expected dependence of $T_g$ on P block molecular weight ($T_{g,P}$ = 71 °C for $M_n$ = 30.1 kg/mol). After vitrification of the P blocks upon cooling, O block crystallization is observed in the range 21 °C $\leq T_{c,O} \leq$ −25 °C using a DSC cooling rate of 5 °C/min; lower values are observed at lower $w_O$. Temperature-dependent SAXS measurements indicate that POP-31-37 and POP-45-25 melt microphase separate into a hexagonal morphology in the range 70 °C $\leq T \leq$ 200 °C, while POP-23-50 is melt-disordered. On the basis of the polymer compositions and the relative stiffness of the P blocks as compared to the O block, we tentatively assign this morphology as a P matrix with O cylinders within which templated O crystallization occurs given that the cylindrical morphology persists in the solid state at 22 °C (Figure 1).[45,46] The melt disordered POP-23-50 exhibits a SAXS pattern with broad scattering maxima consistent with a lamellar morphology at room temperature, which we attribute to crystallization induced segregation of the homogeneous melt.[46−48]

**AOA Triblock Copolymers.** AOA triblock copolymer samples were also opaque and somewhat brittle after aging at 22 °C for 1 day; however, we expected the solid-state morphology of these materials to be different from the POP copolymers due to the known miscibility of A and O homopolymers.[49−53] DSC heating analyses of the aged AOA copolymers reveal a single $T_{g,heat} \sim$ 4−31 °C that monotonically increases with decreasing $w_O$ and a $T_{m,O} \sim 48-58$ °C that monotonically decreases with decreasing $w_O$ (Table 2). $T_{m,O}$ approaches a limiting value of ∼48 °C when $w_O \leq 0.43$ in spite of further increases in $M_{n,A}$ (Figure 2), while $\chi_c$ decreases linearly with decreasing $w_O$ (open circles in Figure 3). Given the trend of increasing $T_{g,heat}$ with decreasing $w_O$, we speculate that $T_{g,heat}$ for AOA-37-30 is masked due to its proximity to $T_{m,O}$. DSC analyses upon cooling the AOA samples with $w_O \leq 0.51$ from the melt show only a single $T_{g,cool} \sim -44$ to −18 °C that increases with decreasing $w_O$ (Table 2 and Supporting Information Figures S4 and S5). No crystallization exotherm is observed for these triblocks at a cooling rate of 5 °C/min when $w_O \leq 0.51$, suggesting that there is a substantial kinetic barrier to O block crystallization. These samples do crystallize slowly over 24 h at 22 °C, and they achieve a maximum crystallinity after 1 day ($\chi_c$ = 0.6−0.7). AOA-37-30 ($w_O$ = 0.30) is exceptional in that it is transparent and tacky after 1 day of aging at 22 °C, and DSC analysis indicates a single $T_g \sim -8$ °C and a weak $T_{m,O} \sim 45$ °C ($\chi_c$ = 0.09). Upon aging for 2 days at 22 °C, the sample crystallizes substantially ($T_{m,O}$ = 48 °C and $\chi_c$ = 0.59), and no $T_{g,heat}$ is observed as noted above (Figure 4).

SAXS analyses were conducted in order to better understand the conditions under which slow crystallization in AOA samples occurs. SAXS patterns acquired for AOA samples in the melt above 60 °C are featureless (Figure 1), consistent with the well-known and well-studied miscibility of the A and O blocks.[49−54] After 1 day of postprocessing aging at 22 °C and attendant O block crystallization, SAXS analyses of AOA samples at 22 °C exhibit a set of weak scattering maxima consistent with a lamellar morphology (Figure 1). Given the single, low $T_{g,cool}$ observed by DSC upon immediately cooling AOA from the melt that is consistent with the miscibility of the A and O blocks, we surmise that O crystallization at 22 °C drives segregation into the observed lamellar morphology as previously observed in polyolefin block copolymers.[47,48] We note that AOA-37-30 exhibits featureless scattering after 1 day of aging at 22 °C, whereas a lamellar morphology is observed after more than 2 days of room temperature aging due to the extraordinarily slow crystallization of this polymer as noted previously.

**BOB Triblock Copolymers.** In stark contrast to the brittle and opaque POP and AOA samples described above, BOB triblock copolymer samples at various compositions range from being qualitatively brittle, opaque materials to ductile, transparent solids upon aging at 22 °C for 1 day. In the aged BOB triblocks with $w_O \geq 0.35$, a single $T_{g,heat} \sim 4$ °C is observed upon heating along with $T_{m,O} \sim 45-49$ °C (Table 3). We also found that $\chi_c$ drops

**Table 2. Characterization Data for AOA Triblock Copolymers**

| sample | $M_{n,A}$ (kg/mol)[a] | $M_{n,\ total}$ (kg/mol) | $M_w/M_n$ | $w_O$ | $T_{m,O}$ (°C)[b] | $T_{g,heat}$ (°C)[c] | $T_{g,cool}$ (°C)[d] | $\chi_c$ |
|---|---|---|---|---|---|---|---|---|
| O[e] | 0 | 11.3 | 1.06 | 1.00 | 58 | −49 | −53 | 0.79 |
| AOA-15-76 | 1.8 | 14.9 | 1.26 | 0.76 | 54 | 4 | n.o.[f] | 0.70 |
| AOA-18-64 | 3.2 | 17.7 | 1.29 | 0.64 | 52 | 14 | n.o.[f] | 0.63 |
| AOA-22-51 | 5.5 | 22.3 | 1.28 | 0.51 | 50 | 15 | −44 | 0.63 |
| AOA-27-43 | 7.6 | 26.5 | 1.19 | 0.43 | 48 | 19 | −34 | 0.60 |
| AOA-29-39 | 9.0 | 29.3 | 1.24 | 0.39 | 49 | 29 | −26 | 0.64 |
| AOA-31-37 | 9.7 | 30.7 | 1.25 | 0.37 | 47 | 31 | −23 | 0.61 |
| AOA-37-30 | 12.9 | 37.1 | 1.34 | 0.30 | 45 | −8 | −18 | 0.09 |
| AOA-37-30 | 12.9 | 37.1 | 1.34 | 0.30 | 48[g] | n.o.[f,g] | −18[g] | 0.59[g] |

[a] Present on each side of the O homopolymer segment. [b] $T_{m,O}$ of O block upon first heating cycle. [c] Observed $T_g$ upon first heating cycle. [d] Observed $T_g$ on first cooling cycle. [e] Difunctional xanthate-terminated O homopolymer **1**. [f] Not observed. [g] After 2 days of aging at 22 °C.

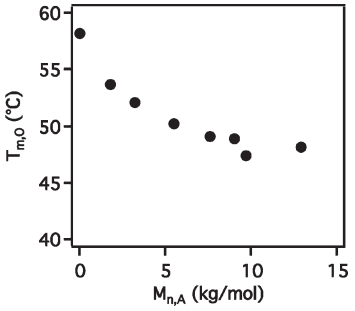


**Figure 2.** Plot of $T_{m,O}$ vs $M_{n,A}$ in AOA samples demonstrating that the observed $T_{m,O}$ declines with increasing $M_{n,A}$, reaching an apparent asymptotic value of 48 °C.

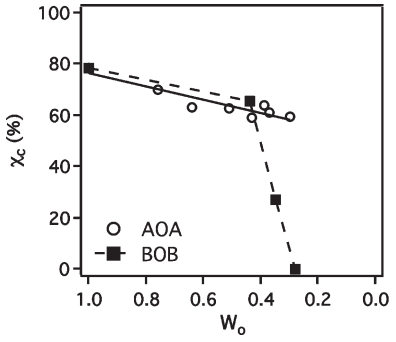


**Figure 3.** Plot of (a) O crystallinity ($\chi_c$) vs mass fraction of O ($w_O$) for AOA samples indicating a linear decrease in $\chi_c$ with decreasing $w_O$ (a best-fit solid line is shown) and (b) $\chi_c$ vs $w_O$ for BOB demonstrating a precipitous decline in $\chi_c$ with decreasing $w_O$ (a dashed line has been added as a guide to the eye).

precipitously with decreasing $w_O$ (Figure 3). When $w_O = 0.28$, we observe $T_{g,heat} \sim 14$ °C and a complete suppression of O crystallinity. Upon immediate cooling from the melt at a rate of 5 °C/min, DSC analyses of all BOB samples reveal a single $T_{g,cool} \sim -27$ to 7 °C that increases with decreasing $w_O$ (see Supporting Information Figures S6 and S7). As with the many of the AOA triblocks, no crystallization exotherm is observed by DSC for any of the BOB triblocks upon immediately cooling the samples from the melt; however, samples with $w_O \geq 0.35$ do crystallize slowly over 1 day of aging at 22 °C.

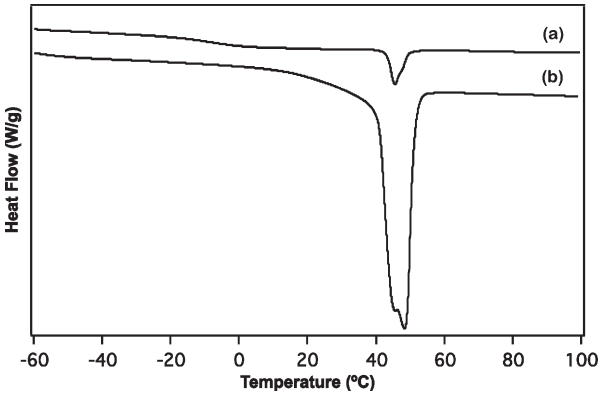


**Figure 4.** DSC heating curves for AOA-37-30 highlighting the difference in $\chi_c$ as a function of postprocessing aging time at 22 °C: (a) 1 day ($\chi_c = 0.09$) and (b) 2 days ($\chi_c = 0.59$).

In order to elucidate the role of block connectivity on BOB polymer thermal properties, a homopolymer blend comprised of macro-RAFT PEO **1** and B homopolymer ($M_n = 17.1$ kg/mol, $M_w/M_n = 1.21$, $T_g = 83$ °C) with $w_O = 0.28$ was studied to emulate the composition of BOB-40-28 and the molecular weights of the homopolymer segments. Analysis of the blend aged at 22 °C for 1 day revealed a melting point $T_{m,O} = 56$ °C that corresponds to the melting transition for semicrystalline O homopolymer, although the presence of B homopolymer does limit the extent of O crystallization to $\chi_c = 0.09$. Two glass transition temperatures were also observed upon heating this blend: $T_g = -44$ °C ascribed to the O homopolymer-rich domains, and a second $T_g = 10$ °C that is attributed to mixed B/O domains. Since $T_g = 83$ °C for neat B homopolymer, a $T_g$ corresponding to pure B homopolymer is not observed in this blend. Figure 5 depicts the DSC heating data for B/O blend after 1 day of aging as compared to BOB-40-28 after aging for 4 months; the latter sample remains amorphous even after such a long aging period. These experiments highlight the fundamental differences between the miscible yet crystallizable B/O homopolymer blend and the completely amorphous BOB triblock copolymers.

SAXS patterns acquired for all of BOB triblock copolymers are apparently featureless above 70 °C, suggesting that the B and O homopolymers are melt miscible. The melt miscibility of this block copolymer was confirmed by rheological measurements on BOB-40-28 that demonstrated that the dynamic elastic storage shear modulus $G'(\omega) \sim \omega^{2.0}$ in the low-frequency regime, as

**Table 3. Characterization Data for BOB Triblock Copolymers**

| sample | $M_{n,B}$ (kg/mol)[a] | $M_{n,\ total}$ (kg/mol) | $M_w/M_n$ | $w_O$ | $T_{m,O}$ (°C)[b] | $T_{g,heat}$ (°C)[c] | $T_{g,cool}$ (°C)[d] | $\chi_c$ |
|---|---|---|---|---|---|---|---|---|
| O[e] | 0 | 11.3 | 1.06 | 1.00 | 58 | −47 | −53 | 0.79 |
| BOB-26-44 | 7.1 | 25.5 | 1.18 | 0.44 | 49 | n.o.[f] | −27 | 0.66 |
| BOB-33-35 | 10.6 | 32.6 | 1.23 | 0.35 | 45 | 4 | −17 | 0.27 |
| BOB-40-28 | 14.3 | 39.9 | 1.26 | 0.28 | n.o.[f] | 14 | 7 | 0 |

[a] Present on each side of the O homopolymer. [b] $T_{m,O}$ of O block upon first heating. [c] Observed $T_g$ upon first heating. [d] Observed $T_g$ on first cooling. [e] Difunctional xanthate-terminated O homopolymer **1**. [f] Not observed.

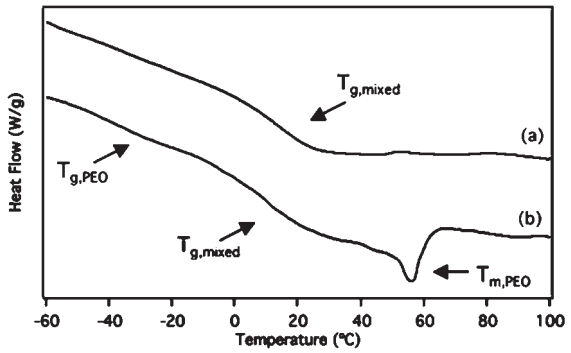


**Figure 5.** DSC heating curves for (a) BOB-40-28 after 4 months of aging at 22 °C ($\chi_c = 0$), indicating the presence of a single $T_g$, and (b) a B/O homopolymer blend (see text for details) after 1 day of aging at 22 °C, demonstrating two distinct $T_g$'s and a melting endotherm associated with semicrystalline O ($\chi_c = 0.09$).

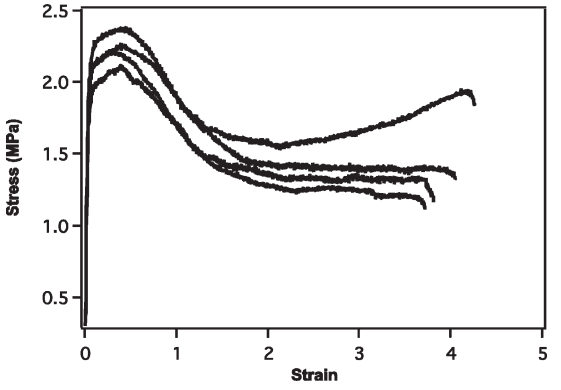


**Figure 6.** Stress vs strain curves for BOB-40-28 demonstrate that the elastic modulus $E = 48.6$ MPa and that a maximum stress at break of $\sigma_{break} = 1.5$ MPa ± 0.3 is achieved at $\varepsilon_{break} = 3.89 \pm 0.30$.

expected for a homogeneous polymer melt.[55] Furthermore, the lack of observable correlation hole scattering above 70 °C by SAXS indicates that these triblocks are quite far from any potential order−disorder transition temperature. After 1 day of aging at 22 °C and attendant O block crystallization, BOB-26-44 ($w_O$ = 0.44) exhibits weak scattering maxima consistent with a lamellar morphology resulting from a crystallization-induced segregation as seen in the AOA samples. BOB-33-35 and BOB-40-28, however, display no obvious SAXS scattering maxima even after 1 day of aging at 22 °C.

**Mechanical Properties of BOB-40-28 and B/O Blend.** While the crystallizable BOB samples exhibited brittle behavior, the observed ductility of the completely amorphous BOB-40-28 motivated studies of its uniaxial tensile properties. During these tests, rectangular samples were strained using a length independent strain rate of 0.01 $s^{-1}$. Clear, flexible samples plaques of BOB-40-28 deformed uniformly upon loading with no signs of neck formation upon drawing. The samples begin to strain whiten nonuniformly in small areas of the gauge section at 250−300% strain. Further elongation causes the samples to become uniformly translucent. Stress−strain curves for BOB-40-28 are shown in Figure 6. Analysis of the linear regime of the observed stress−strain curves ($\varepsilon < 5.0\%$) revealed an elastic modulus $E = 48.6 \pm 4.4$ MPa. The ultimate tensile strength of BOB-40-28 was $\sigma_{break} = 1.5 \pm 0.3$ MPa at a maximum elongation of $\varepsilon_{break} = 3.89 \pm 0.3$; however, these values are at best lower bounds on the ultimate properties of these materials as three out of four sample broke at the tensile tester grips. Upon breaking, the samples recover to ∼150% of their original length over the course of hours, during which time they further whiten and become completely opaque. Uniaxial tensile tests conducted on the compositionally identical B/O homopolymer blend, however, demonstrated its brittle properties with $\varepsilon_{break} < 0.10$. (A representative stress−strain curve for the B/O homopolymer blend is given in Supporting Information Figure S8.)

## DISCUSSION

Poly(vinyl ester)/PEO triblock copolymers POP, AOA, and BOB exhibit three very different solid state morphologies that arise directly from the relative chemical compatibilities of the constituent homopolymer blocks and the thermal transitions that occur upon cooling from the melt. The presence of poly(vinyl ester) end blocks flanking the crystallizable O block hampers O crystallization as compared to compositionally similar homopolymer blends;[53,56] however, the intimate differences in phenomena for these blends and block copolymers have not been previously investigated. The three scenarios that we observed correspond to (i) crystallization within a microphase-separated melt in POP, (ii) crystallization-induced segregation in AOA, and (iii) partial or complete suppression of crystallization in BOB. We interpret the results of our studies and their attendant consequences for the mechanical properties of these block copolymers within this conceptual framework.

Because of the high degree of chemical incompatibility between the P and O blocks, the POP triblock copolymers microphase separate at temperatures up to 200 °C into a hexagonally packed cylinders morphology. Cooling these microphase-separated melts results in initial vitrification of the glassy P blocks ($T_g \sim 47-61$ °C) followed by O block crystallization ($T_{c,O} \sim 21$ to −25 °C). Given that $T_{m,O} \sim 45-58$ °C upon heating, the large degree of O block supercooling in POP triblocks prior to crystallization implies that there is a kinetic barrier to O crystallization at low O contents. This effect likely stems from the triblock copolymer architecture in which the crystallizable block is constrained at two domain interfaces. The observed melting temperatures and crystallinities

for the microphase-separated samples are consistent with prior reports of confined O crystallization in strongly segregated microphase diblock copolymers,[57,58] in which crystal thickness is limited by lateral crystal growth along the long axis of the cylinders with the crystal stems oriented perpendicular to the domain interface. Not surprisingly, arranging semicrystalline O cylinders within a glassy P matrix results in a mechanically brittle material due to the lack of soft domains that can accommodate tensile loading.[59]

SAXS analyses of AOA triblock copolymer melts indicate that these materials are melt disordered due to the known miscibility of A and O homopolymers.[51] Thus, the observed O crystallization occurs from a homogeneous polymer melt. The presence of the A blocks reduces the resulting crystallinity and crystal thickness in the O domains as compared to the parent homopolymer **1**, as indicated by the lower crystalline weight fractions and the depressed O melting temperatures. Crystallization-induced segregation in these materials drives the formation of a lamellar morphology, although there is a substantial kinetic barrier to O crystallization that mandates the aging of samples at 22 °C for at least 24 h to achieve maximum crystallinity. This long crystallization time scale hampers direct observation of the crystallization temperature $T_{c,O}$ by DSC when $w_O \leq 0.51$. The apparent kinetic barrier to O crystallization increases dramatically as $M_{n,A}$ increases, given that AOA-37-30 requires at least 2 days of room temperature aging to crystallize maximally due to the high viscosity of the single-phase melt upon cooling which impedes crystal nucleation and growth.

The observation of two glass transition temperatures $T_{g,heat}$ and $T_{g,cool}$ upon heating and cooling AOA triblock copolymers reflects the state of the polymer melt under different circumstances. Because of the slow crystallization of the O segments from the homogeneous polymer melt, $T_{g,cool}$ likely reflects the $T_g$ of the miscible A/O melt.[51] Consistent with this notion is the fact that $-44\ °C \leq T_{g,cool} \leq -18\ °C$ and $T_{g,O} = -53\ °C$ for O homopolymer **1**, where $T_{g,cool}$ shifts to higher temperatures with decreasing O content. The higher $T_{g,heat}$ observed upon heating AOA triblock copolymers corresponds to the glass transition temperature of the A-rich domains within the lamellar morphology induced by crystallization from the homogeneous melt; the increasing $T_{g,heat}$ correlates well with increasing A content ($T_{g,A} \sim 40\ °C$). Ultimately, the layered lamellar structure comprised of glassy A blocks and highly crystalline O blocks results in a brittle mechanical response.

BOB triblock copolymers exhibit a range of composition-dependent thermal properties that correlate with the level of O crystallinity in the block copolymer. Surprisingly, B and O homopolymers are melt-miscible as indicated by SAXS and rheological analyses above 70 °C (vide supra). Thus, crystallization in BOB-26-44 and BOB-33-35 occurs from a homogeneous melt and should result in a lamellar solid-state morphology due to crystallization-induced segregation as in the AOA samples. SAXS data support the notion that the substantially crystalline BOB-26-44 adopts a lamellar morphology, while BOB-33-35 shows no obvious scattering maxima and only low O block crystallinity. The crystalline BOB triblocks also exhibit two different $T_g$'s upon heating and cooling, a situation analogous to that of the AOA triblock copolymers in which crystallization-induced segregation creates O-rich and B-rich domains from the miscible melt.

The unusual mechanical properties of BOB-40-28 originate from the completely amorphous center O segment of this block copolymer. Below a threshold value in the range $w_O = 0.28-0.35$, O crystallization is completely inhibited even after 4 months of aging at 22 °C. By comparison to a B/O homopolymer blend with $w_O = 0.28$ and with B and O molecular weights comparable to those of the segments in the block copolymer that exhibits $\chi_c = 0.09$, we see that the *inhibition of crystallization arises as a direct consequence of the triblock copolymer chain architecture*. The solid appearance of these samples and their mechanical properties imply that there may be a glass transition temperature slightly above room temperature that is not detectable by DSC upon heating at variable heating rates, even after various annealing protocols.[60] On this basis, we speculate that the slow segmental dynamics of B segments within the intimately mixed O and B domains completely inhibit crystallization. By virtue of the suppression of O crystallization, the BOB triblock acts as a glassy–amorphous–glassy triblock copolymer in which the amorphous, entangled O block ($M_{e,O} \sim 1.7$ kg/mol) imparts ductility and the glassy domains pin these amorphous entanglements in a molecular "block and tackle" arrangement.[28,35,59] Thus, the amorphous BOB-40-28 behaves like a weak thermoplastic with a low level of elastic recovery, while the compositionally similar B/O homopolymer blend is brittle as are the low molecular weight B and O homopolymers by themselves. The mechanical properties of amorphous BOB-40-28 are comparable to those of recently reported microphase-separated poly(styrene-*b*-butyl acrylate-*b*-styrene) elastomers.[61] Surprisingly, we find that the expected number of entanglements in the center block of the aforementioned microphase-separated styrene/acrylate block copolymers and the number of amorphous O entanglements in completely amorphous BOB-40-28 are comparable. This suggests that trapped entanglements play a primary role in determining the mechanical properties of these triblock copolymer materials regardless of the mode of microphase separation.

## CONCLUSION

The thermal, morphological, and mechanical properties of POP, AOA, and BOB triblock copolymers comprised of an 11.3 kg/mol O center segment flanked by glassy poly(vinyl ester) blocks have been examined, in an attempt to toughen brittle poly(vinyl ester) homopolymers through the incorporation of a low entanglement molecular weight center segment. These polymers are of potential interest for use in degradable packaging applications and in biomedical devices given the known biocompatibility and degradability of the O and the poly(vinyl ester) blocks, respectively. These three homologous triblock copolymers exhibit three very different solid-state mechanical behaviors that depend sensitively on the sequence of thermal transitions upon cooling from the melt, especially, O block crystallization. POP triblock copolymers melt microphase separate and O block crystallization is confined within the domains of the supramolecular morphology, resulting in a brittle mechanical response arising from enchainment of glassy P blocks with highly crystalline O blocks. In contrast to this case, O crystallization in the AOA and BOB systems occurs from a single-phase (homogeneous) melt. AOA triblock copolymers undergo a kinetically slow crystallization-induced segregation to form a lamellar morphology that exhibits a brittle solid-state behavior. BOB triblock copolymers undergo a similar crystallization-induced segregation unless the weight fraction of O drops below $w_O < 0.30$, at which point crystallization is completely inhibited. The inhibition of crystallization imparts the BOB triblock copolymer with $w_O = 0.28$ with unusual ductility and some degree of reversible elasticity. Studies of BOB triblock copolymers having variable O block molecular weights and compositions are underway to elucidate

the roles of suppressed O crystallization, strain-induced crystallization, and O block entanglement on the mechanical properties of these new materials.

## ■ ASSOCIATED CONTENT

**Supporting Information.** Sample SEC traces for representative triblock copolymers and DSC heating and cooling traces for all triblock copolymers. This material is available free of charge via the Internet at http://pubs.acs.org.

## ■ AUTHOR INFORMATION

**Corresponding Author**
*E-mail: mahesh@chem.wisc.edu.

## ■ ACKNOWLEDGMENT

This work was funded by the National Science Foundation (NSF CAREER DMR-0748503) and the Wisconsin Alumni Research Foundation. This research also made extensive use of UW-Madison MRSEC/NSEC characterization facilities (DMR-0520527 and DMR-0425880). We also thank Professors Wendy Crone and Kristyn Masters for assistance with tensile testing experiments.

## ■ REFERENCES

(1) Ober, C. K.; Cheng, S. Z. D.; Hammond, P. T.; Muthukumar, M.; Reichmanis, E.; Wooley, K. L.; Lodge, T. P. *Macromolecules* **2009**, *42*, 465.
(2) Avella, M.; De Vlieger, J. J.; Errico, M. E.; Fischer, S.; Vacca, P.; Volpe, M. G. *Food Chem.* **2005**, *93*, 467.
(3) Drumright, R. E.; Gruber, P. R.; Henton, D. E. *Adv. Mater.* **2000**, *12*, 1841.
(4) Gruber, P.; O'Brien, M. *Biopolymers* **2002**, *4*, 235.
(5) Anderson, K. S.; Schreck, K. M.; Hillmyer, M. A. *Polym. Rev.* **2008**, *48*, 85.
(6) Shin, J.; Martello, M. T.; Shrestha, M.; Wissinger, J. E.; Tolman, W. B.; Hillmyer, M. A. *Macromolecules* **2011**, *44*, 87.
(7) Cohn, D.; Hotovely Salomon, A. *Biomaterials* **2005**, *26*, 2297.
(8) Gautrot, J. E.; Zhu, X. X. *Angew. Chem., Int. Ed.* **2006**, *45*, 6872.
(9) Lendlein, A.; Neuenschwander, P.; Suter, U. W. *Macromol. Chem. Phys.* **1998**, *199*, 2785.
(10) Moravek, S. J.; Hassan, M. K.; Drake, D. J.; Cooper, T. R.; Wiggins, J. S.; Mauritz, K. A.; Storey, R. F. *J. Appl. Polym. Sci.* **2010**, *115*, 1873.
(11) Jeon, O.; Lee, S.-H.; Kim, S. H.; Lee, Y. M.; Kim, Y. H. *Macromolecules* **2003**, *36*, 5585.
(12) Wanamaker, C. L.; Tolman, W. B.; Hillmyer, M. A. *Biomacromolecules* **2009**, *10*, 443.
(13) Zhou, C.; Leng, B.; Yao, J.; Qian, J.; Chen, X.; Zhou, P.; Knight, D. P.; Shao, Z. *Biomacromolecules* **2006**, *7*, 2415.
(14) Coulembier, O.; Mespouille, L.; Hedrick, J. L.; Waymouth, R. M.; Dubois, P. *Macromolecules* **2006**, *39*, 4001.
(15) Chen, W.; Meng, F.; Li, F.; Ji, S.-J.; Zhong, Z. *Biomacromolecules* **2009**, *10*, 1727.
(16) Wang, L.-S.; Cheng, S.-X.; Zhuo, R.-X. *Macromol. Rapid Commun.* **2004**, *25*, 959.
(17) Schreck, K. M.; Hillmyer, M. A. *J. Biotechnol.* **2007**, *132*, 287.
(18) Daniels, W. E. *Vinyl Ester Polymers in Encyclopedia of Polymer Science and Engineering*, 2nd ed.; Mark, H. F., Ed.; Wiley: New York, 1985; Vol. 17, p 393.
(19) Marten, F. L. *Vinyl Alcohol Polymers in Encyclopedia of Polymer Science & Engineering*, 2nd ed.; Mark, H. F., Ed.; Wiley: New York, 1985; Vol. 17, p 167.
(20) Chiellini, E.; Corti, A.; D'Antone, S.; Solaro, R. *Prog. Polym. Sci.* **2003**, *28*, 963.
(21) Matsumura, S. *Biopolymers* **2003**, *9*, 329.
(22) Lipscomb, C. E.; Mahanthappa, M. K. *Macromolecules* **2009**, *42*, 4571.
(23) Bunck, D. N.; Sorenson, G. P.; Mahanthappa, M. K. *J. Polym. Sci., Part A: Polym. Chem.* **2011**, *49*, 242.
(24) Repollet-Pedrosa, M. H.; Weber, R. L.; Schmitt, A. L.; Mahanthappa, M. K. *Macromolecules* **2010**, *43*, 7900.
(25) Lipscomb, C. E.; Mahanthappa, M. K. *Polym. Prepr.* **2010**, *51*, 233.
(26) Lipscomb, C. E.; Mahanthappa, M. K., unpublished results.
(27) Holden, G.; Bishop, E. T.; Legge, N. R. *J. Polym. Sci., Part C* **1969**, *26*, 37.
(28) Holden, G.; Legge, N. R.; Quirk, P. R.; Schroeder, H. E. *Thermoplastic Elastomers*, 2nd ed.; Hanser Publishers: New York, 1996.
(29) Séguéla, R.; Prud'homme, J. *Macromolecules* **1981**, *14*, 197.
(30) Kawai, H.; Hashimoto, T.; Miyoshi, K.; Uno, H.; Fujimura, M. *J. Macromol. Sci., Phys.* **1980**, *B17*, 427.
(31) Bates, F. S.; Fredrickson, G. H.; Hucul, D. A.; Hahn, S. F. *AIChE J.* **2001**, *47*, 762.
(32) Holden, G.; Legge, N. R. In *Thermoplastic Elastomers*; Holden, G., Legge, N. R., Quirk, P. R., Schroeder, H. E., Eds.; Hanser: Munich, 1996; p 47.
(33) Pakula, T.; Saijo, K.; Kawai, H.; Hashimoto, T. *Macromolecules* **1985**, *18*, 1294.
(34) Cohen, Y.; Albalak, R. J.; Dair, B. J.; Capel, M. S.; Thomas, E. L. *Macromolecules* **2000**, *33*, 6502.
(35) Lim, L. S.; Harada, T.; Hillmyer, M. A.; Bates, F. S. *Macromolecules* **2004**, *37*, 5847.
(36) Tong, J.-D.; Jerome, R. *Macromolecules* **2000**, *33*, 1479.
(37) Fetters, L. J.; Lohse, D. J.; Colby, R. H. Chain dimensions and entanglement spacings. In *Physical Properties of Polymers Handbook*; Mark, J. E., Ed.; Springer Science & Business Media, LLC: New York, 2006; p 445.
(38) Reid, B.; Tzeng, S.; Warren, A.; Kozielski, K.; Elisseeff, J. *Macromolecules* **2010**, *43*, 9588.
(39) Malepu, V.; Petruczok, C. D.; Tran, T.; Zhang, T.; Thopasridharan, M.; Shipp, D. A. *ACS Symp. Ser.* **2009**, *1024*, 37.
(40) Destarac, M.; Charmot, D.; Franck, X.; Zard, S. Z. *Macromol. Rapid Commun.* **2000**, *21*, 1035.
(41) Pound, G.; Aguesse, F.; McLeary, J. B.; Lange, R. F. M.; Klumperman, B. *Macromolecules* **2007**, *40*, 8861.
(42) Wunderlich, B. *Macromolecular Physics*; Academic Press: New York, 1980; Vol. 3.
(43) Tong, Y.-Y.; Dong, Y.-Q.; Du, F.-S.; Li, Z.-C. *J. Polym. Sci., Part A: Polym. Chem.* **2009**, *47*, 1901.
(44) Lee, J.-Y.; Tan, B.; Cooper, A. I. *Macromolecules* **2007**, *40*, 1955.
(45) Quiram, D. J.; Register, R. A.; Marchand, G. R. *Macromolecules* **1997**, *30*, 4551.
(46) Loo, Y.-L.; Register, R. A.; Ryan, A. J. *Macromolecules* **2002**, *35*, 2365.
(47) Rangarajan, P.; Register, R. A.; Fetters, L. J. *Macromolecules* **1993**, *26*, 4640.
(48) Koo, C. M.; Wu, L.; Lim, L. S.; Mahanthappa, M. K.; Hillmyer, M. A.; Bates, F. S. *Macromolecules* **2005**, *38*, 6090.
(49) Zhao, J.; Zhang, L.; Ediger, M. D. *Macromolecules* **2008**, *41*, 8030.
(50) Urakawa, O.; Ujii, T.; Adachi, K. *J. Non-Cryst. Solids* **2006**, *352*, 5042.
(51) Gaikwad, A. N.; Wood, E. R.; Ngai, T.; Lodge, T. P. *Macromolecules* **2008**, *41*, 2502.
(52) Tyagi, M.; Arbe, A.; Alegria, A.; Colmenero, J.; Frick, B. *Macromolecules* **2007**, *40*, 4568.
(53) Fragiadakis, D.; Runt, J. *Macromolecules* **2010**, *43*, 1028.
(54) Chen, X.; An, L.; Li, L.; Yin, J.; Sun, Z. *Macromolecules* **1999**, *32*, 5905.
(55) Hiemenz, P. C.; Lodge, T. P. *Polymer Chemistry*, 2nd ed.; CRC Press: Boca Raton, 2007; p 444.

(56) Wu, L.; Lisowski, M.; Talibuddin, S.; Runt, J. *Macromolecules* **1999**, *32*, 1576.
(57) Chu, C.-Y.; Chen, H.-L.; Hsiao, M.-S.; Chen, J.-H.; Nandan, B. *Macromolecules* **2010**, *43*, 3376.
(58) Zhu, L.; Cheng, S. Z. D.; Calhoun, B. H.; Ge, Q.; Quirk, R. P.; Thomas, E. L.; Hsiao, B. S.; Yeh, F.; Lotz, B. *Polymer* **2001**, *42*, 5829.
(59) Mahanthappa, M. K.; Lim, L. S.; Hillmyer, M. A.; Bates, F. S. *Macromolecules* **2007**, *40*, 1585.
(60) The small discrepancy in $T_{g,heat}$ and $T_{g,cool}$ for BOB-40-28 is attributed to some hysteresis upon cooling.
(61) Luo, Y.; Wang, X.; Zhu, Y.; Li, B.-G.; Zhu, S. *Macromolecules* **2010**, *43*, 7472.